F. Boukhili[1,*]
A. Zaafouri [2]
M.A Dami [2]

J. Electrical Systems 18-2 (2022): 246-259

Regular paper

JES
Journal of Electrical Systems

# 3-Phase Induction motor speed control based space vector modulation technique for direct matrix converter under unbalanced conditions

In this work, the performance analysis and discussion of a space vector modulation technique used for a three-phase direct matrix converter feeding a three-phase induction motor is presented. For this, the induction motor models and the method of the space vector modulation technique are developed. Then, the overall electrical drive system is simulated using MatLab/Simulik software. Results obtained from simulation are the harmonic spectrum analysis of the motor current and the total harmonic distortion for unbalanced input voltages. These results show the good performance of the control system strategy.

Keywords: Direct matrix converter; Induction-motor; SVM algorithm, Harmonics Distortion.

## 1. Introduction

Advances in power electronics have enabled the development of a new generation of static power converters to drive various industrial applications, including renewable energy and variable speed power generation [1, 2].

Indeed, the variable speed drives offer significant advantages such as the rationalization of the energy expenses, the motors' consumption which is strictly necessary for the application, on the power supply network This reasonable electric consumption eliminates at the time of starting the strong amplitudes of the currents called asynchronous motors. In addition, the matrix converter (MC) controlled in this study has several advantages over conventional converters.

Indeed, for a sinusoidal input, a sinusoidal output waveform is provided, with a minimum of harmonics, thanks to the inherent possibilities of bidirectional energy flow.

The input power factor can be fully controlled. It requires minimal energy storage, which allows it to get rid of the clutter and limited energy storage time of capacitors. However, the matrix converter requires powerful control algorithms to manage the switching of the switches. The maximum voltage transfer ratio is limited to ≅ 87% for an output and input sinusoidal-shaped. It requires more semiconductor devices than the conventional indirect converter.

Several modulation algorithms are developed to control the various bidirectional switches of the direct type matrix converter. Among these different control strategies are Venturini, scalar and space vector modulation (SVM algorithms.)

Pulse modulated voltage inverters (PWM) are very interesting for researchers. They have used it especially for the AC machines. There are several methods of controlling these converters. Among them, two control variants stand out: sinusoidal pulse width modulation (SPWM) [1, 3] and space vector pulse width modulation (SVPWM) [4, 5]. It is certain that the choice of a better inverter control strategy, feeding a three-phase asynchronous machine with cage, improves considerably the system performances

[*] Corresponding author: Boukhili Farhat , *ISET, Jendouba*, *ENSIT, LISIER Laboratory*, *Jendouba, Tunisia*, E-mail: boukhilifarhat@yahoo.fr

[1] *ISET, Jendouba*, *ENSIT, LISIER Laboratory*, *Jendouba, Tunisia*
[2] *ENSIT, Tunis*, ENSIT, LISIER Laboratory, *Tunis, Tunisia*

For this reason, we adopt vector modulation, which has the advantage of minimizing current harmonics, reducing torque pulses and ensuring a higher modulation index (15%). The load current is sinusoidal and the current source does not contain only high and multiples harmonics of the sampling frequency [3, 4].
It allows the adjustment of the displacement factor of the current source, which reduces the reactive power consumption and therefore optimizes the size and power of the installed equipment.
The following parts of the paper are organized as follows: section 2 presents the mathematical model of the AC induction motor. In Section 3, we develop the adopted control strategy of the direct matrix converter. Section 4 is devoted to the simulation results and discussion of the technical performance in the case of balanced and unbalanced states. In section 5, we highlight a conclusion.

## 2. Design and modeling of the control method

Fig. 1 represents the induction motor and the matrix converter which is controlled with SVM method.

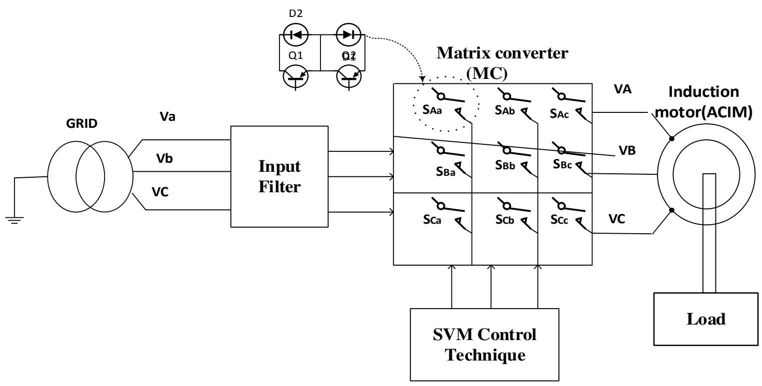


Figure.1: Block Diagram of DMC-IM

### *2.1. Mathematic model of the doubly fed induction motor*

In the reference "dq" the components of the stator and rotor voltages are written by (1) and (2), respectively [7-9]:

$$\begin{cases} V_{sd} = R_s.I_{sd} + \dfrac{d\varphi_{sd}}{dt} - \omega_s.\varphi_{sq} \\ V_{sq} = R_s.I_{sq} + \dfrac{d\varphi_{sq}}{dt} + \omega_s.\varphi_{sd} \end{cases} \quad (1)$$

$$\begin{cases} V_{rd} = R_r.I_{rd} + \dfrac{d\varphi_{rd}}{dt} - (\omega_s - \omega_r).\varphi_{sq} \\ V_{rq} = R_r.I_{rq} + \dfrac{d\varphi_{rq}}{dt} + (\omega_s - \omega_r).\varphi_{sd} \end{cases} \tag{2}$$

**Where**

$v_{ds}, v_{qs}$: d-axis , q-axis stator voltage respectively;
$v_{ds}, v_{qr}$: d-axis , q-axis rotor voltage ;
$I_{ds}, I_{qs}$: d-axis , q-axis stator current ;
$I_{dr}, I_{qr}$: d-axis , q-axis rotor current;
$\lambda_{ds}, \lambda_{qs}$: d-axis, q-axis stator fluxes;
$\lambda_{dr}, \lambda_{qr}$: d-axis, q-axis rotor fluxes;
$r_s, r_r$: stator and rotor resistance;
$\omega_s$: Rotational speed of synchronous reference.

Where the flux components are given as follow:

$$\begin{cases} \varphi_{sd} = L_s I_{sd} + M I_{rd} \\ \varphi_{sq} = L_s I_{sq} + M I_{rq} \\ \varphi_{rd} = L_r I_{rd} + M I_{sd} \\ \varphi_{rq} = L_r I_{sq} + M I_{rq} \end{cases} \tag{3}$$

Where , $L_s = L_{ls} + M$ and $L_r = L_{lr} + M$ .

Hence, the representation as state space is:

$$\begin{bmatrix} V_{sd} \\ V_{sq} \end{bmatrix} = \begin{bmatrix} R_s & 0 \\ 0 & R_s \end{bmatrix} \begin{bmatrix} i_d \\ i_q \end{bmatrix} \frac{d}{dt} \begin{bmatrix} \varphi_{sd} \\ \varphi sq \end{bmatrix} + \begin{bmatrix} 0 & \omega_s \\ \omega_s & 0 \end{bmatrix} \begin{bmatrix} \varphi_{sd} \\ \varphi_{sq} \end{bmatrix} \tag{4}$$

$$\begin{bmatrix} \varphi_{sd} \\ \varphi_{sq} \\ \varphi_{rd} \\ \varphi_{rq} \end{bmatrix} = \begin{bmatrix} L_s & 0 & M & 0 \\ 0 & L_s & 0 & M \\ M & 0 & L_r & 0 \\ 0 & M & 0 & L_r \end{bmatrix} \begin{bmatrix} i_{sd} \\ i_{sq} \\ i_{rd} \\ i_{rq} \end{bmatrix} \tag{5}$$

And, the equation of dynamic motion and electromagnetic torque are given, respectively, in the following expressions:

$$J.\frac{d\Omega}{dt} = T_{em} - Tr - f\Omega \quad where \quad \Omega = \frac{w}{p} \tag{6}$$

$$T_{em} = p(\varphi_{sq}.I_{sd} - \varphi_{sd}.I_{sq}) \tag{7}$$

$T_{em}$: electromagnetic torque;
$T_r$: load torque;

*p*: number of pole pairs;
*J*: moment of inertia;
Ω: rotational speed.

### *2.2. Matrix converter modeling*

The matrix converter (MC) is an AC/AC converter made of nine (9) bidirectional switches. The Matrix Converter of 3x3 switches ( see Fig. 2) has the highest practical interest because it connects a three-phase voltage source with a three-phase load. With the initial progress made by Venturini, it has received considerable attention in recent years [10].

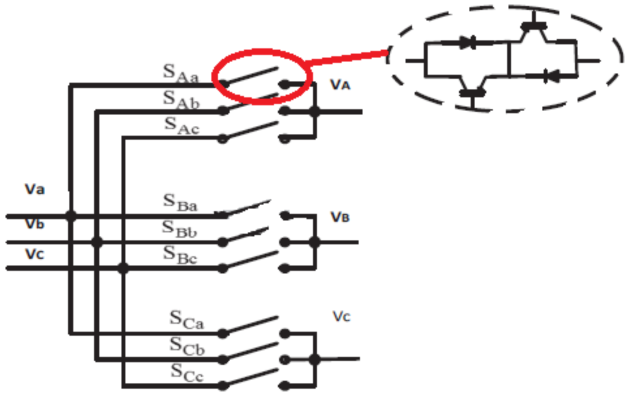


Fig. 2. Matrix converter structure.

The bidirectional power switches operate with high switching frequency. A low frequency output voltage of variable amplitude and frequency can be generated by modulating the duty cycle of the switches using their respective switching functions. The MC has 27 possible switching states and the switching function of every switch is defined by [11].

$$S_{kj} = \begin{cases} 0 & if \quad S_{kj} \quad is\ open \\ 1 & if \quad S_{kj} \quad is\ closed \end{cases} \tag{9}$$

Where, $k$=A, B, C and $j$=a,b,c.

The constraints discussed above can be expressed as follow:

$$S_{Aj} + S_{Bj} + S_{Cj} = 1 \tag{10}$$

The MC connects any input phase (A, B, and C) to any output phase (a, b, and c) at any instant. When connected, the voltages $v_{an}$, $v_{bn}$, $v_{cn}$ at the output terminals are related to the input voltages $V_{Ao}$, $V_{Bo}$, $V_{Co}$ . The input and output quantities of the considered MC are, mathematically, related to each other by the connecting matrix. The use of this matrix leads to the equations written by (11) and (12).

$$\begin{bmatrix} V_{an} \\ V_{bn} \\ V_{cn} \end{bmatrix} = \begin{bmatrix} S_{Aa} & S_{Ba} & S_{Ca} \\ S_{Ab} & S_{Bb} & S_{Cb} \\ S_{Ac} & S_{Bc} & S_{Cc} \end{bmatrix} \begin{bmatrix} V_{Ao} \\ V_{Bo} \\ V_{Co} \end{bmatrix} \tag{11}$$

Where, $S_{Aa}$ through $S_{Cc}$ are the switching variables.

The three phase-to-phase voltage systems $V_{AB}$, $V_{BC}$, $V_{CA}$ are the components of a voltage vector $\overrightarrow{V_0}$ defined by the relation:

$$\overrightarrow{V_0} = \frac{2}{3}\left(V_{AB} + e^{\frac{j2\pi}{3}}.V_{BC} + e^{\frac{-j2\pi}{3}}.V_{CA}\right) = \|V_0\|.e^{j\theta} \quad (12)$$

By the way, the input phases currents ($i_e$) are expressed in the following matrix form:

$$\begin{bmatrix} i_A \\ i_B \\ i_C \end{bmatrix} = \begin{bmatrix} S_{Aa} & S_{Aa} & S_{Aa} \\ S_{Bb} & S_{Bb} & S_{Bb} \\ S_{Cc} & S_{Cc} & S_{Cc} \end{bmatrix} \begin{bmatrix} i_a \\ i_b \\ i_c \end{bmatrix} \quad (13)$$

Furthermore,

$$\overrightarrow{i_e} = \frac{2}{3}\left(I_a + e^{\frac{j2\pi}{3}}.I_b + e^{\frac{-j2\pi}{3}}.V_c\right) = |I_e|.e^{j\varphi} \quad (14)$$

## 2. Description of SVM control method

The concept of vector modulation (SVM) is generally used for inverter control and then applied to matrix converters. This approach is based on the spatial vector representation of the output voltage vector ($\overrightarrow{V_0}$) and the input current vector ($\overrightarrow{i_e}$) in the dq frame. The space vector is obtained from the Concordia transform.

Vector modulation consists in synthesizing output voltages from input voltages and input currents from output currents.

In the Space Vector approach, the 27 possible switching combinations are divided into three groups. Out of the three groups only 21 places for useful space vectors (18 of which are non-zero and 3 are zero). Fig.2.8a shows the output voltage vector and Fig.2.8b shows the input current vectors. KV denotes the output voltage vector sector and KI denotes the input current vector sector. The output phases are indicated by a, b, and c, and the input phases are indicated by A, B, and C. Based on equations (12) and (14), we can draw the following table used in the SVM [11 , 12, 13].

Table.1.The different possible configurations

| **Configuration** | | **Switechs closed** | $\|V_0\|$ | $\theta$ | $\|I_e\|$ | $\varphi$ |
|---|---|---|---|---|---|---|
| $abb$ | $+1$ | $S_{aA}S_{bB}S_{bC}$ | $\frac{2}{\sqrt{3}}.U_{AB}$ | $\frac{\pi}{6}$ | $\frac{2}{\sqrt{3}}I_A$ | $-\frac{\pi}{6}$ |
| $baa$ | $-1$ | $S_{bA}S_{aB}S_{aC}$ | $\frac{2}{\sqrt{3}}U_{AB}$ | $-5\frac{\pi}{6}$ | $\frac{2}{\sqrt{3}}I_A$ | $5\frac{\pi}{6}$ |

| | | | | | | |
|---|---|---|---|---|---|---|
| $bcc$ | $+2$ | $S_{bA}S_{cB}S_{cC}$ | $\frac{2}{\sqrt{3}}U_{BC}$ | $\frac{\pi}{6}$ | $\frac{2}{\sqrt{3}}I_A$ | $\frac{\pi}{2}$ |
| $cbb$ | $-2$ | $S_{cA}S_{bB}S_{bC}$ | $\frac{2}{\sqrt{3}}U_{BC}$ | $-5\frac{\pi}{6}$ | $\frac{2}{\sqrt{3}}I_A$ | $-\frac{\pi}{2}$ |
| $caa$ | $+3$ | $S_{cA}S_{aB}S_{aC}$ | $\frac{2}{\sqrt{3}}U_{CA}$ | $\frac{\pi}{6}$ | $\frac{2}{\sqrt{3}}I_A$ | $-5\frac{\pi}{6}$ |
| $acc$ | $-3$ | $S_{aA}S_{cB}S_{cC}$ | $\frac{2}{\sqrt{3}}U_{CA}$ | $-5\frac{\pi}{6}$ | $\frac{2}{\sqrt{3}}I_A$ | $\frac{\pi}{6}$ |
| $bab$ | $+4$ | $S_{bA}S_{aB}S_{bC}$ | $\frac{2}{\sqrt{3}}U_{AB}$ | $5\frac{\pi}{6}$ | $\frac{2}{\sqrt{3}}I_B$ | $-\frac{\pi}{6}$ |
| $aba$ | $-4$ | $S_{aA}S_{bB}S_{aC}$ | $\frac{2}{\sqrt{3}}U_{AB}$ | $-\frac{\pi}{6}$ | $\frac{2}{\sqrt{3}}I_B$ | $5\frac{\pi}{6}$ |
| $cbc$ | $+5$ | $S_{cA}S_{bB}S_{cC}$ | $\frac{2}{\sqrt{3}}U_{BC}$ | $5\frac{\pi}{6}$ | $\frac{2}{\sqrt{3}}I_B$ | $\frac{\pi}{2}$ |
| $bcb$ | $-5$ | $S_{bA}S_{cB}S_{bC}$ | $\frac{2}{\sqrt{3}}U_{BC}$ | $-\frac{\pi}{6}$ | $\frac{2}{\sqrt{3}}I_B$ | $-\frac{\pi}{2}$ |
| $aca$ | $+6$ | $S_{aA}S_{cB}S_{aC}$ | $\frac{2}{\sqrt{3}}U_{CA}$ | $5\frac{\pi}{6}$ | $\frac{2}{\sqrt{3}}I_B$ | $-5\frac{\pi}{6}$ |
| $cac$ | $-6$ | $S_{cA}S_{aB}S_{cC}$ | $\frac{2}{\sqrt{3}}U_{CA}$ | $-\frac{\pi}{6}$ | $\frac{2}{\sqrt{3}}I_B$ | $\frac{\pi}{6}$ |
| $bba$ | $+7$ | $S_{bA}S_{bB}S_{aC}$ | $\frac{2}{\sqrt{3}}U_{AB}$ | $-\frac{\pi}{2}$ | $\frac{2}{\sqrt{3}}I_C$ | $-\frac{\pi}{6}$ |
| $aab$ | $-7$ | $S_{aA}S_{aB}S_{bC}$ | $\frac{2}{\sqrt{3}}U_{AB}$ | $\frac{\pi}{2}$ | $\frac{2}{\sqrt{3}}I_C$ | $5\frac{\pi}{6}$ |
| $ccb$ | $+8$ | $S_{cA}S_{cB}S_{bC}$ | $\frac{2}{\sqrt{3}}U_{BC}$ | $-\frac{\pi}{2}$ | $\frac{2}{\sqrt{3}}I_C$ | $\frac{\pi}{2}$ |
| $bbc$ | $-8$ | $S_{bA}S_{bB}S_{cC}$ | $\frac{2}{\sqrt{3}}U_{BC}$ | $\frac{\pi}{2}$ | $\frac{2}{\sqrt{3}}I_C$ | $-\frac{\pi}{2}$ |
| $aac$ | $+9$ | $S_{aA}S_{aB}S_{cC}$ | $\frac{2}{\sqrt{3}}U_{CA}$ | $-\frac{\pi}{2}$ | $\frac{2}{\sqrt{3}}I_C$ | $-5\frac{\pi}{6}$ |
| $cca$ | $-10$ | $S_{cA}S_{cB}S_{aC}$ | $\frac{2}{\sqrt{3}}U_{CA}$ | $\frac{\pi}{2}$ | $\frac{2}{\sqrt{3}}I_C$ | $\frac{\pi}{6}$ |
| $aaa$ | 01 | $S_{aA}S_{aB}S_{aC}$ | 0 | --- | 0 | --- |
| $bbb$ | 02 | $S_{bA}S_{bB}S_{bC}$ | 0 | --- | 0 | --- |
| $ccc$ | 03 | $S_{cA}S_{cB}S_{cC}$ | 0 | --- | 0 | --- |

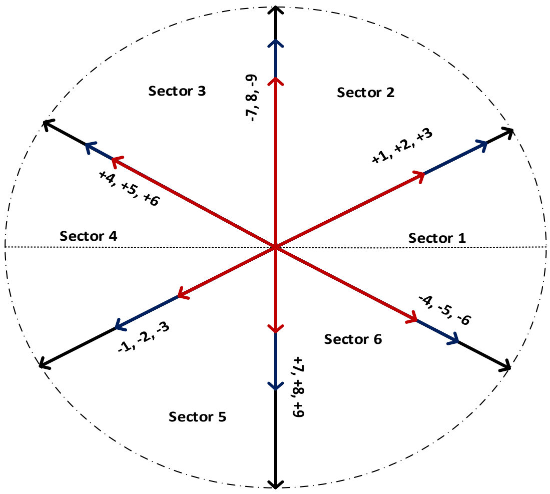


Figure. 3. Voltage's plan.

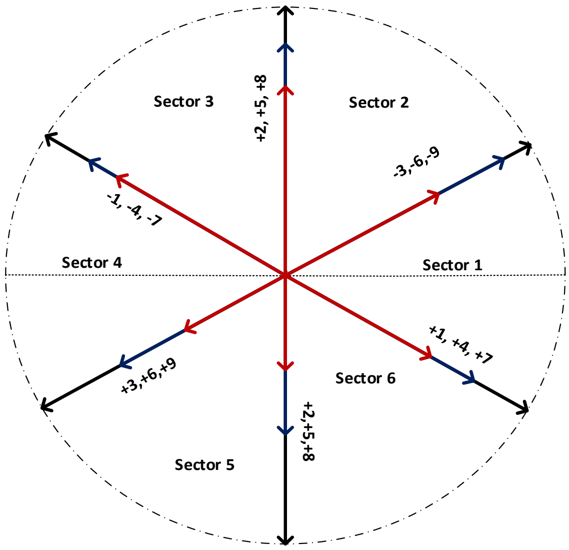


Figure. 4. Current's plan

## 4. Simulation results

The system studied above consists of a three-phase induction motor driven by a matrix converter. So, the SVM method applied at matrix converter-DMC drive has been simulated using the MatLab/Simulink package program. Subsequently, simulation results are presented to verify and validate the proposed structure of control.

In order not to encumber the content of this work, only two main cases related to the behavior of phase_a are highlighted in this study (first phase) stator. At the begining, the network parameters (amplitude and phase) are considered nominal after the case where the phase_a under goes a decrease of 25% of its nominal amplitude. Finally, the corresponding results are analyzed and discussed. However, Figures (5 to 12) and (13 to 18) represent, respectively, the results of simulations when the parameters are nominal (reference case) and the phase_a imbalance case. Those results represent, each in turn, the shapes of the voltages of the network (a) which are directly connected to the stator of the induction asynchronous motor, the shapes of the voltages at the output of the matrix converter ,the speed , the torque , the stator currents and finally the spectral analysis of the current of the stator phases.

Analysis of the results shows that the case of unbalanced voltages remarkably affects the operating behavior of the motor for the control structure of a ACIM-matrix converter electric drive. Oscillations occur in speed and torque. The rate of distortion harmonics is remarkable. This fact therefore, requires sophisticated and high-performance controls of the assembly to make an insensitive system.

- In the case of balanced voltages

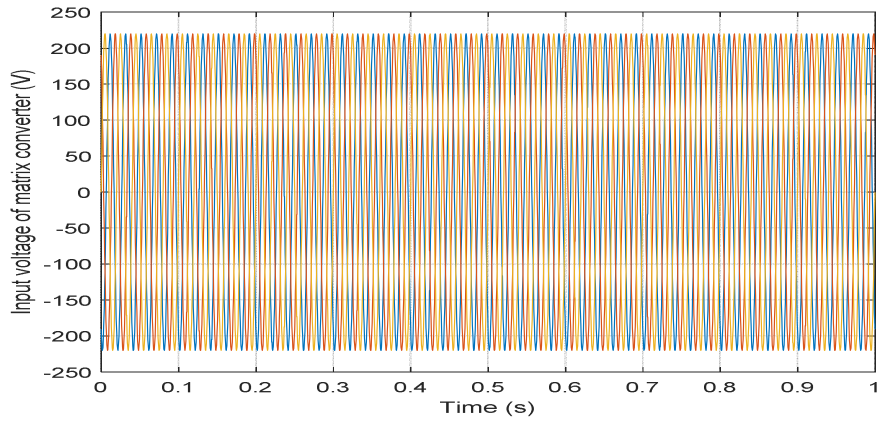


Figure. 5. Balanced voltages.

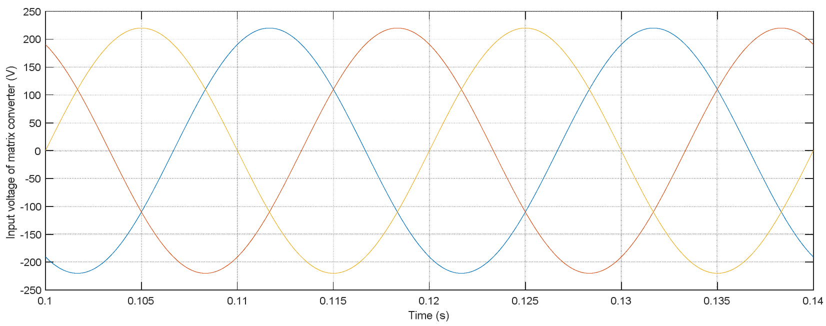


Figure. 6. Input voltage of matrix converter

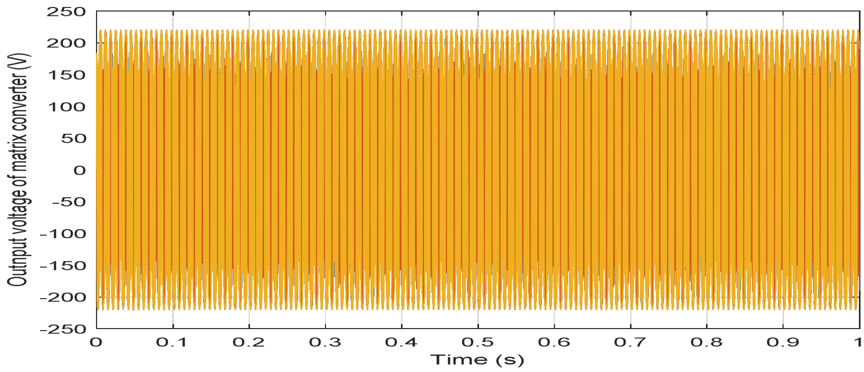


Figure. 7. Stator voltages.

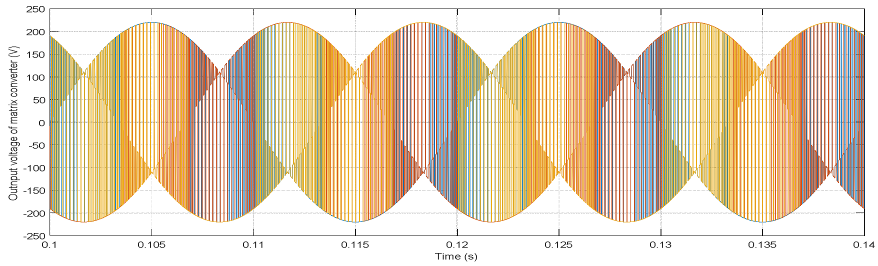


Figure. 8. Output voltage of matrix converter

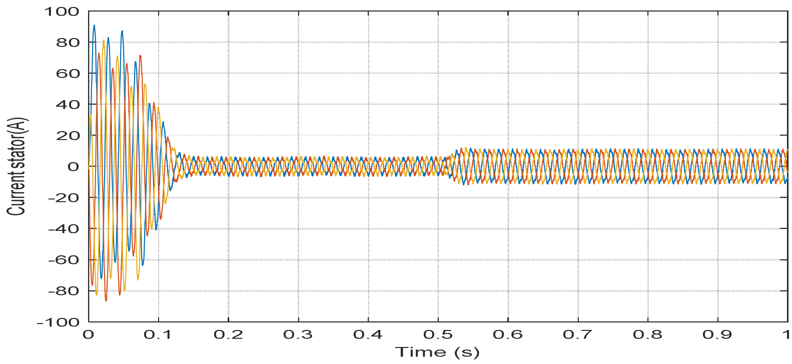


Figure. 9. Phase's currents.

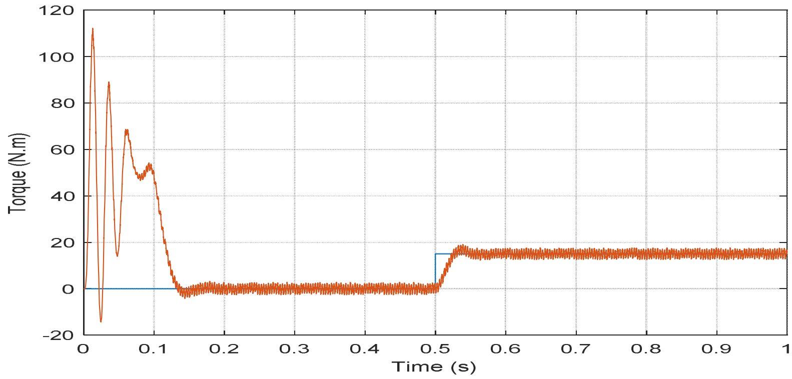


Figure. 10. Motor's torque

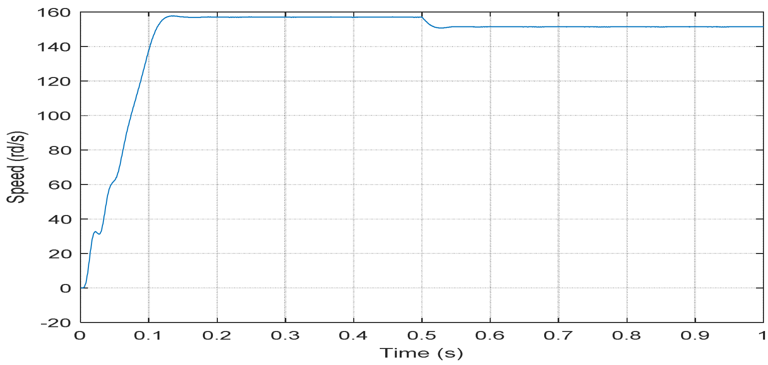


Figure. 11. Motor's speed

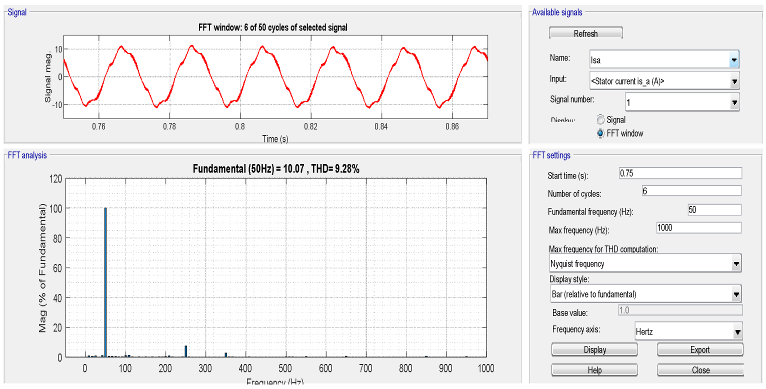


Figure. 12. Characteristic performances under nominal conditions.

- In the case of unbalanced voltages amplitude (220v,200v,180v)

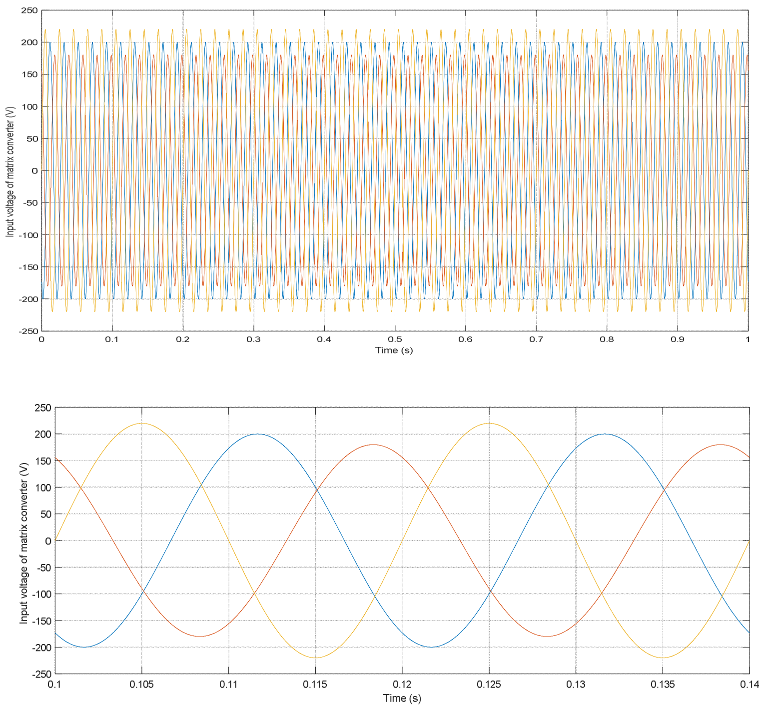


Figure. 13.  Input voltages of matrix converter

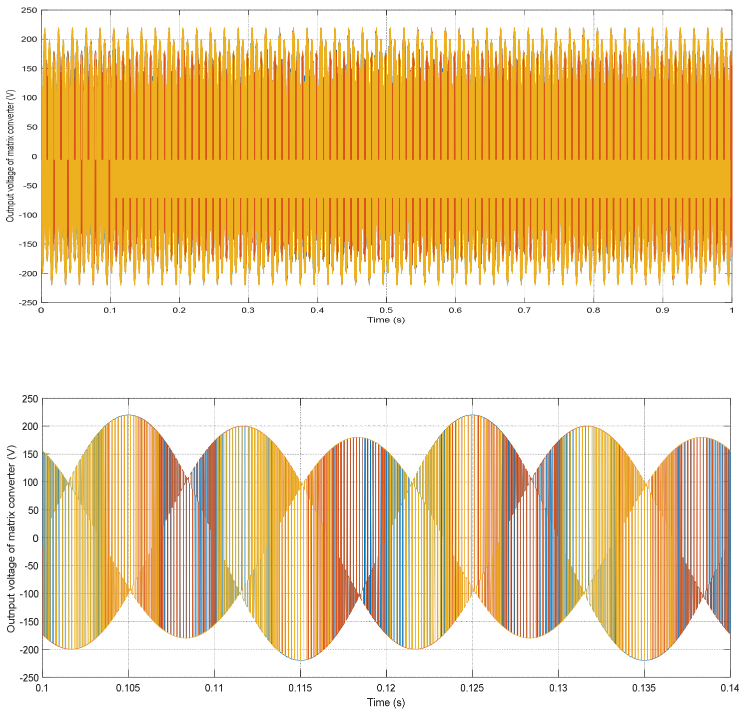


Figure. 14. Output voltages of matrix converter

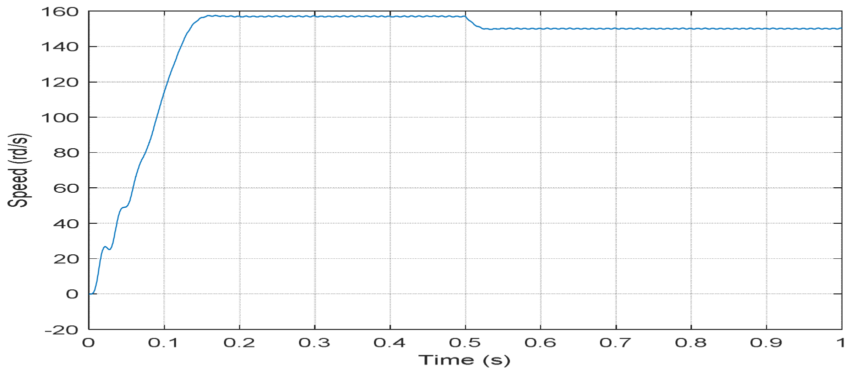


Figure. 15. Motor speed

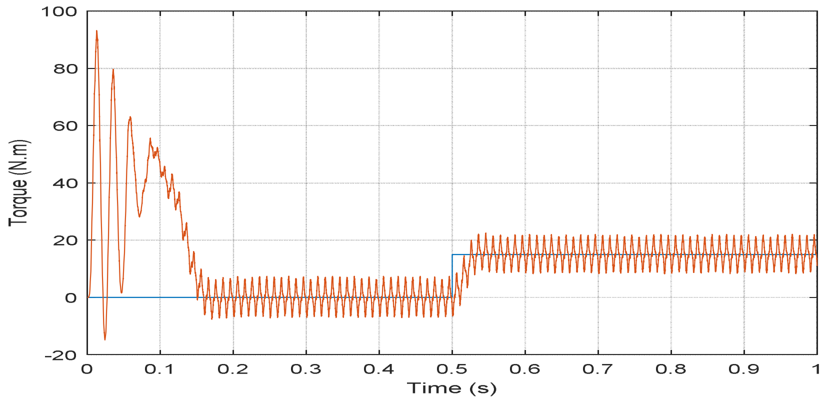


Figure. 16. Electromagnetic torque and reference.

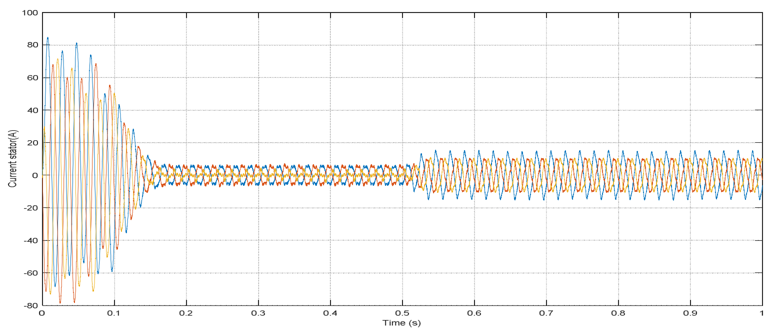


Figure.17. Current's stator

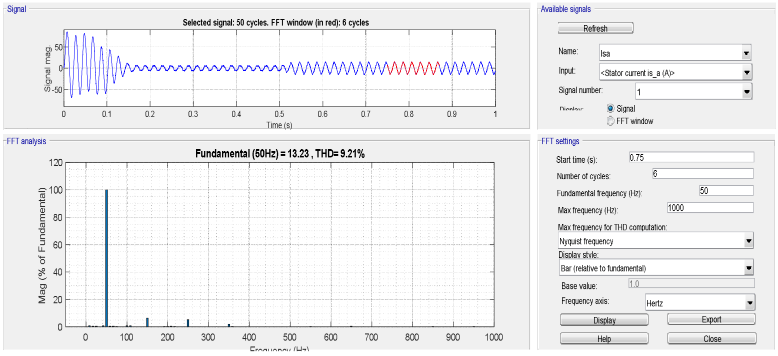


Fig. 18. Characteristic performances under unbalanced conditions

## 6. Conclusion

The performance analysis of a control system consisting of a three-phase induction motor fed by a direct matrix converter controlled by space vector modulation was the subject of this work. In addition, the operation with a power supply at nominal parameters, which is the case of unbalanced stator phase voltages, has also been considered. The analysis shows that such structure inevitably requires adequate controls in order to reduce the impact of unbalance on the motor behavior and to improve the performance of the whole system.

## 7. Reference

[1] Dr. S. Srinath, Mrs. S. Poongothai, T. Aruna, "PV integration shunt active filter for harmonic compensation," 1st International conference on power engineering, computing and control, peccon-2017, 2-4 March 2017, VIT University, Chennai Campus. Science Direct, Energy Procedia 117 (2017) 1134-1144.

[2] Moh. Jauhari, Dedet Candra Riawan, Mochamad Ashari," Control Design for Shunt Active Power Filter Based on p-q Theory in Photovoltaic Grid-Connected System", International Journal of Power Electronics and Drive System (IJPEDS) Vol. 9, No. 3, September 2018, pp.1064~1071.

[3] M. Kala, N. Rathina Prabha., " Grid Interconnected Photovoltaic System Using Shunt Active Filter for Power Quality Improvement, "International Journal of Power Electronics and Drive Systems (IJPEDS), vol. 9, pp. 365-376, 2018.

[4] Arpit Shah, Nirav Vaghela "Shunt Active Power Filter for Power Quality Improvement in Distribution Systems", International Journal of Engineering Development and Research 2005, ISSN: 2321-9939.

[5] Neha Kumari, Isha Awashthi,"Harmonic Compensation Using Shunt Active Power Filter in Power System Using Matlab", International Journal of Scientific Engineering and Research. ISSN (Online): 2347-3878Vol. 1 Issue 3, November 2013.

[6] M. Thousif, S Sumukha, Ashwini G and Ankitha R," Modelling and Simulation of Shunt Active Filter for Harmonic Reduction", International Journal of Engineering Research & Technology, ISSN: 2278-0181-2017 Conference Proceedings

[7] M. Deben Singh, , R. K. Mehta , A. K. Singh," Performance assessment of current source converter based UPQC for power quality improvement with simple control strategies", J. Electrical Systems 15-2 (2019): 276-290

[8] B. Boukezata, A. Chaoui, J.P. Gaubert, and M. Hachemi "Photovoltaic solar system connected to the electrical network and associated with a parallel active filter," Electrical Engineering Symposium, Cachan, 2014.

[9] Petit, F. J. Robles, Guillermo. Amarís, Hortensia, "Current Reference Control for Shunt Active Power Filters under Nonsinusoidal Voltage Conditions," IEEE Transactions on Power Delivery, vol. 22, no. 4, hal. 2254-2261, 2007.

[10] M. I. Montero, E.R. Kadaval, F. B. Gonzalez, "Comparison of Control Strategies for Shunt ActivePower Filters in Three-Phase Four-Wire Systems," IEEE Trans. On Power Elec., vol. 22, no. 1, 2007.

[11] H.J.Azevedo, J.M. Ferreira, A.P. Martins, and A.S. Carvalho "Direct current control of an active power filter for harmonic elimination, power factor correction and load unbalancing compensation", Proceedings of the 10th European Conference on Power Electronics and Applications, EPE'03,Toulouse, 2003, pp. 1-10

[12] V N Jayasankar1, U Vinatha," Advanced Control Approach for Shunt Active Power Filter Interfacing WindSolar Hybrid Renewable System to Distribution Grid", J. Electrical Systems 14-2 (2018): 88-102.

[13] Ramos Hernanz, JA. Campayo Martin,JJ. Zamora Belver,I., Larranga Lesaka,J. , Zulueta Guerrero,E. p "Modelling of photovoltaic module", International Conference on Renewable Energies and Power Quality (ICREPQ'10) Granada (Spain), 23th to 25th March, 2010.

[14] Huan-Liang Tsai, Ci-Siang Tu, and Yi-Jie Su, Member, IAENG, "Development of generalized photovoltaic model using MATLAB /SIMULINK", Proceedings of the World Congress on Engineering and Computer Science 2008,WCECS 2008, October 22 - 24, 2008, San Francisco, USA .

[15] M.G. Villalva, J.R. Gazoli and E.R. Filho, "Comprehensive approach to modeling and simulation of photovoltaic array", IEEE Trans on Power Electronics, Vol. 24, n°5, pp. 1198-1208,May 2009 .

[16] Roberto Faranda, Sonia Leva "Energy Comparison of MPPT techniques for PV Systems" WSEAS Transactions on Power Systems, June 2008.

[17] Yuvarajan and Shanguang Xu," Photovoltaic Power Converter with a Simple Maximum Power Point Tracker", IEEE 2003.

[18] J. M. Enrique, J. M. Andujar, and M. a. Bohorquez, "A reliable, fast and low cost maximum power point tracker for photovoltaic applications," Solar Energy, vol. 84, no. 1, pp. 79–89, 2010.

[19] T.Chaitanya, Ch.Saibabu, J.Surya Kumari "Modeling and Simulation of PV Array and its Performance Enhancement Using MPPT (P&O) Technique", International Journal of Computer Science & Communication Networks,Vol 1(1),September-October 2011.

[20] Nicola Femia, Member IEEE "Optimization of Perturb and Observe Maximum Power Point Tracking Method", IEEE 2005.

[21] Emílio F. Couto, Júlio S. Martins, João L. Afonso, «Simulation Results of a Shunt Active Power Filter with Control Based on p-q Theory", International Conference on Renewable Energies and Power Quality Vigo, Espanha, 9-12 de Abril de 2003, paper 394, ISBN: 84 607 6768.

[22] G. Dan, D. Benjamin, R. Magureanu, L. Asiminoaei, R. Teodorescu, and F. Blaabjerg, "Control strategies of active filters in the context of power conditioning", European Conference on Power Electronics and Applications, 2005.

[23] A.P.Martins, "The use of an active power filter for harmonic elimination and power quality improvement in a nonlinear loaded electrical installation", Proceedings of the International Conference on Renewable Energies and Power Quality, ICREPQ'03, Vigo, 2003, pp.1-6.

[24] K. Hasan, and K. Osman, "Globally Stable Control of Three-Phase Three Wire Shunt Active Power Filters", Elec. Eng., Vol.89, no.5, 2007, pp.411-418.